Catalysis Communications 157 (2021) 106333

Contents lists available at ScienceDirect

Catalysis Communications

journal homepage: www.elsevier.com/locate/catcom

Short communication

Aerobic iron-catalyzed site-selective C(sp^3)–C(sp^3) bond cleavage in *N*-heterocycles

David K. Leonard, Wu Li, Nils Rockstroh, Kathrin Junge, Matthias Beller *

Leibniz-Institut für Katalyse e.V., Albert-Einstein-Straße 29a, 18059 Rostock, Germany

ARTICLE INFO

Keywords:
Iron
Oxidation
C–C bond activation
Design of experiments

ABSTRACT

The kinetic and thermodynamic stability of C(sp^3)–C(sp^3) bonds makes the site-selective activation of these motifs a real synthetic challenge. In view of this, herein a site-selective method of C(sp^3)–C(sp^3) bond scission of amines, specifically morpholine and piperazine derivatives, using a cheap iron catalyst and air as a sustainable oxidant is reported. Furthermore, a statistical design of experiments (DoE) is used to evaluate multiple reaction parameters thereby allowing for the rapid development of a catalytic process.

1. Introduction

Iron is the most abundant metal in the universe, and due to its propensity towards oxidation it is found in the earth's crust as one of its several ores, namely hematite (Fe_2O_3), magnetite (Fe_3O_4), and siderite ($FeCO_3$). In the field of catalysis, no base metal has impacted the world quite like iron; in fact, heterogeneous iron catalysis has triumphed in some of the world's most important industrial processes [1]. For instance, the Fischer−Tropsch process has established itself as an indispensable technology for the synthesis of liquid hydrocarbons and has been implemented by leading petrochemical companies. Undoubtedly, the Haber−Bosch process has had the most significant impact since its introduction in 1913 at BASF. At present this remains the leading industrial method for artificial nitrogen fixation, producing ammonia from N_2 and H_2, and is a vital technology for securing global food production. Notably, both revolutionary processes utilize iron-based catalysts [2–4].

The contemporary literature has often highlighted the talents of iron for enabling an extensive range of organic transformations [5–7]. Thanks to its position in the center of the 3d block of the periodic table, iron may be considered by chemists as either an *early* or *late* transition metal, and due to its formal oxidation states, which range from −2 to +6, it has a vast potential for all kinds of redox transformations [1,8–11]. New applications for iron are eagerly sought after, especially in the field of catalysis, thanks to its ready availability, low cost, and typically low toxicity.

1.1. C(sp^3)–C(sp^3) bond activation

There is an ongoing surge in new methodologies for the activation of C(sp^3)–C(sp^3) bonds which are ubiquitous within the framework of organic compounds [12–17]. Due to their kinetic and thermodynamic stability, traditional methods—such as the Criegee [18] and Malaprade [19] reactions—are ill-suited transformations for organic compounds bearing sensitive functional motifs. For this reason there has been an aim towards realizing mild reaction conditions and greater functional group tolerance. With this goal in mind, our group was able to establish a copper-mediated system for the cleavage of C(sp^3)–C(sp^3) bonds in amines [20]. Following this initial report, we developed an improved bimetallic cobalt−manganese system with activity and selectivity towards the cleavage of morpholine derivatives [21]. Although we were able to shift to more earth-abundant metals, we were intrigued to utilize cheap and non-toxic iron for such transformations (Fig. 1).

1.2. Experimental design

Compared to classic optimization strategies, statistical design of experiments (DoE) has gained increasing reputation among industrial chemists in recent years as an effective methodology for reaction optimization and identification of critical reaction parameters [22,23]. More specifically, this paradigm shift is a result of:

1. the development of parallel reactors, high-throughput experimentation (HTE) and flow reactor setups having been implemented widely,

* Corresponding author.
E-mail address: matthias.beller@catalysis.de (M. Beller).

https://doi.org/10.1016/j.catcom.2021.106333
Received 17 March 2021; Received in revised form 8 June 2021; Accepted 16 June 2021
Available online 18 June 2021

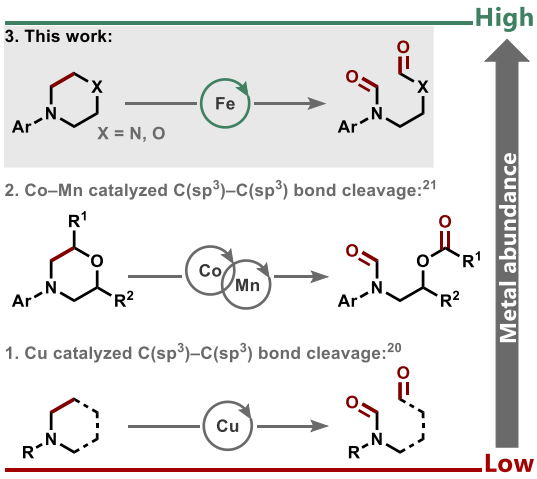

Fig. 1. Selected recent methods of metal catalyzed oxidative C–C bond cleavage reactions [20,21], and this work: iron-catalyzed C–C bond cleavage.

2. the shift away from quality by testing towards the adoption of quality by design (QbD), with the concept of design space becoming more widely known,
3. the Green Chemistry Principles [24] having encouraged chemists to reduce waste output from chemical reactions and increase efficiency by reducing the amounts of solvents and reagents used in chemical processes.

Interestingly, DoE tools are not widely adopted in academia despite their advantages. In contrast to univariate—i.e. linear, or one-factor-at-a-time (OFAT)—analyses, multivariate approaches to experimental design allow expansive areas of chemical space to be explored in an efficient and expedient manner [25].

Since many factors can influence the outcome of a chemical reaction (e.g. conversion, yield, selectivity, byproduct formation), DoE can be an invaluable addition to the synthetic chemist's toolbox. Not only can DoE cut down on the number of experimental runs used in optimization, but it also allows significant factors—and interactions between factors—to be identified; this is simply not feasible using a one-factor-at-a-time approach. What's more, DoE can streamline the process of locating the global maximum response for a reaction (i.e. the conditions furnishing the most desirable outcome) by investigating multiple dimensions simultaneously (as illustrated in Fig. 2).

In an effort to expand upon our previous methodologies, and building more sustainable practices, we herein report a new catalytic system for the site-selective cleavage of C(sp^3)–C(sp^3) bonds in (cyclic) amines.

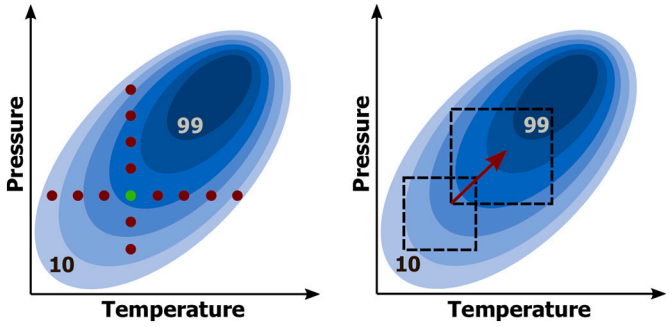

Fig. 2. Comparison between a univariate OFAT study (two sequential studies, first exploring T, then *p*) (left) and a multivariate full-factorial study (one study exploring T and *p* at the same time) for a hypothetical reaction. Dark blue regions indicate more desirable responses. (For interpretation of the references to colour in this figure legend, the reader is referred to the web version of this article.)

DoE was used for efficient optimization of the reaction by mapping of chemical space, analyzing multiple variables simultaneously. Advantageously, not only were we able to employ a very cheap, readily available, and "biocompatible" iron catalyst but also utilize air as the most green and sustainable oxidant. Notably, oxidation reactions in aerated solvents inherently possess significant safety concerns, which must be addressed appropriately. Indeed, organic chemists in academia but also the pharmaceutical industry in particular try to avoid such synthetic steps [28]. Starting materials tend therefore to be acquired in at least the correct (or higher) oxidation levels. This can certainly generate an additional hurdle in route design, and thus new practical methodologies are readily sought to address this [29]. On the other hand it's true that aerobic oxidations are applied in several large and medium scale industrial processes, which demonstrates the possibilities to perform such transformations in a selective, safe, and environmentally benign manner [26,27]. In our case, safety concerns were in large part circumvented by using (synthetic) air which uses diluted oxygen in inert nitrogen, as well as oxidation resistant solvents.

2. Experimental

2.1. General experimental details

Most substrates were obtained from commercial sources and used as supplied; others were prepared as detailed below.

All metal catalysts were obtained from commercial sources and used as supplied.

Unless otherwise mentioned, all catalytic oxidation reactions were carried out in 2 mL glass vials, which were set in an alloy plate and placed inside a 300 mL autoclave (Parr® Instrument Company).

All oxidation reactions were performed in a Parr® Instrument Company autoclave.

Deuterated solvents were ordered from Deutero GmbH. NMR spectra were recorded using Bruker 300 Fourier, Bruker AV 300 and Bruker AV 400 spectrometers. Chemical shifts are reported in ppm, relative to the deuterated solvent. Coupling constants are expressed in Hertz (Hz). The following abbreviations are used: s = singlet, d = doublet, t = triplet, and m = multiplet. The residual solvent signals were used as references for ^{1}H and ^{13}C NMR spectra ($CDCl_3$: δH = 7.26 ppm, δC = 77.12 ppm; DMSO-d_6: δH = 2.50 ppm, δC = 39.52 ppm). All measurements were carried out at room temperature unless otherwise stated.

GC-FID analyses were carried out using an Agilent 7890B gas chromatograph fitted with an Agilent HP5 column (30 m × 0.25 mm I.D. x 0.25 μm).

Solvents were used directly without further purification. HPLC grade MeCN was supplied by Fisher Chemical.

Scanning transmission electron microscopy (STEM) was performed with a probe aberration-corrected JEM-ARM200F (Jeol Ltd., CEOS Corrector) at 200 kV. The microscope is further equipped with an Enfinium ER (Gatan) electron energy loss spectrometer. For STEM imaging a High-Angle Annular Dark Field (HAADF) and an Annular Bright Field (ABF) detector were applied, while EELS acquisition was done with the Annular Dark Field (ADF) detector. The solid sample was dried in advance of the electron microscopy measurements and then placed without any further pretreatment on a holey carbon supported Cu-grid (mesh 300), which was then transferred to the microscope. EEL spectra were background subtracted and deconvolved.

2.2. General procedure for the synthesis of substrates

2.2.1. General procedure A (GP-A)

A mixture of aryl bromide (10 mmol), morpholines (20 mmol), K_2CO_3 (20 mmol), CuI (1.0 mmol) and L-proline (2.0 mmol) in 10 mL of DMSO was heated at 90 °C and for 24 h. The cooled mixture was partitioned between water and ethyl acetate. The organic layer was separated, and the aqueous layer was extracted with ethyl acetate. The

combined organic layers were dried over Na_2SO_4, and concentrated in vacuo. The desired products were isolated by silica gel column chromatography (*n*-heptane/ethyl acetate mixtures) [34].

2.3. General procedure for catalytic oxidations

2.3.1. General procedure B (GP-B)

A 4 mL glass vial equipped with a magnetic stir bar was charged with aryl morpholine (0.5 mmol) and $FeCl_3$ (8.1 mg; 10 mol%). The vial was capped, and the septum was pierced with a small needle. HPLC grade acetonitrile (2 mL) was added via a 2 mL syringe. Pyridine (80 μL; 2.0 equiv) was added via a glass microsyringe. The vial was then placed into an aluminium heating block and then sealed inside an autoclave (Parr® Instrument Company). The autoclave was then pressurized with air (30 bar). The reaction mixture was stirred for 24 h at 100 °C. Next, the reaction was cooled to room temperature. A sample of the reaction mixture was analyzed by GC-FID and TLC. The product was purified via flash column chromatography (RediSep® Rf + automatic column) using heptane/ethyl acetate. Solvent was removed in vacuo to yield the desired product.

2.3.2. General procedure C (GP-C)

A 4 mL glass vial equipped with a magnetic stir bar was charged with 1,4-diphenylpiperazine (59.6 mg; 0.25 mmol), TEMPO (3.9–11.7 mg; 10–30 mol%) and $FeCl_3$ (2.0–6.1 mg; 3–15 mol%) in that order. The vial was capped, and the septum was pierced with a small needle. HPLC grade acetonitrile (1 mL) was added via a 2 mL syringe. Pyridine (2.0–6.0 μL; 10–30 mol%) was added via a glass microsyringe. The vial was then placed into an aluminium heating block and then sealed inside an autoclave (Parr® Instrument Company). The autoclave was then pressurized with air (10–30 bar). The reaction mixture was stirred for 24 h at 80–120 °C. Next, the reaction was cooled to room temperature. A sample of the reaction mixture was analyzed by GC-FID and yield was determined using *n*-hexadecane as an internal standard (see appendix for GC-FID calibration graphs). Product isolation was achieved via flash column chromatography (RediSep® Rf + automatic column) using a suitable mixture of heptane/ethyl acetate determined by TLC. Solvent was removed in vacuo to yield the desired product.

3. Results and discussion

To develop our expertise in the area of base metal-catalyzed C(sp^3)–C(sp^3) bond cleavage reactions, we investigated various metal salts for the cleavage of *N*-phenylmorpholine **1a** under aerobic conditions [20,21]. In addition to our recently published [Cu]/air and [Co–Mn]/air systems, several iron catalysts showed promising activity for this transformation (Table S3).

The most favorable results were obtained using iron(III) chloride (entry 7), although lower yields could also be obtained using iron(III) nitrate nonahydrate (entry 5) and iron(II) phthalocyanine (entry 6). Encouraged by these initial findings we opted to compare the performance of the catalyst in various solvents (see Table S4) and found that acetonitrile proved to be the most effective solvent, which is consistent with our previously disclosed catalytic systems [20,21]. At this point it is important to note that the use of organic solvents in oxidation reactions is always potentially hazardous; especially performing reactions under aerobic conditions without appropriate safety measures. Hence, we completed all experiments in standard autoclave equipment with synthetic air as the oxidant—which contains just 20.5 ± 0.5% O_2 diluted in N_2 gas—as an operationally safer system to pure O_2. In addition, we used solvents with high resistance to autooxidation. Notably, the chosen solvent, acetonitrile, has an autoignition temperature of 524 °C, as well as lower and upper explosive limits of 4.4 and 16%, respectively (see safety data sheets) [30], which allows for safe and reproducible work under our reaction conditions. It should be also mentioned that in all experiments we never observed any evidence of solvent oxidation.

Unlike our recently reported [Co–Mn]/air system, iron(III) chloride was able to perform oxidative cleavage outwith the class of morpholines (Table 1). The catalyst's activity towards 1,4-diphenylpiperazine (**2a**) under the pre-optimized conditions using (2,2,6,6-tetramethyl-piperidin-1-yl)oxyl (TEMPO)—a stable free radical reagent—was particularly encouraging. It is noteworthy to point out that the presence of pyridine ligands highly influenced the yield of **2b** (Table 1); a documented effect of *N*-ligands in oxidations [20,21,31,32]. However, a reproducible positive effect was only observed in the presence of the parent ligand. Pyridines both substituted with electron-donating as well as electron-withdrawing substituents gave inferior results.

In contrast to our previously reported systems for C–C single bond cleavage, which showed high activity towards a variety of amines (in the case of [Cu]) and functionalized morpholines (in the case of [Co–Mn]), with this new $FeCl_3$ catalyst system, better performance was obtained with piperazine substrates. Notably, the [Co–Mn] system was found to be completely ineffective with such substrates.

With a suitable catalyst, solvent and additives in hand for site-selective C(sp^3)–C(sp^3) bond cleavage in **2a** to **2b**, we postulated that a DoE methodology is a suitable tool for establishing a more realistic process. It is expected that the reaction parameters: catalyst loading, temperature, air pressure, pyridine loading, and TEMPO loading could all significantly influence the reaction yield of **2b** (Table 2).

The rationale behind the ranges of the low-level (−) and high-level conditions (+) of the selected variables is that they must be large enough to ensure any effects on reaction yield should be easily detectable. Additionally, using a wide range between these two values is one of the best ways to improve the signal/noise ratio. A two-level half-fractional (2^{5-1}) factorial design was selected to enable a large area of chemical space to be covered whilst keeping the number of experimental runs to a minimum and avoid compounding effects.

Using a software statistics package (Minitab) [33], we generated a list of all necessary experimental runs to cover the chosen design space. Included in the design are four runs in the center of the design space (9 mol% catalyst loading, 100 °C, 20 bar air, 20 mol% pyridine, 20 mol% TEMPO), leading to a total of twenty experimental runs. The yield of **2b** in each run was determined by gas chromatograph-flame ionization detector (GC-FID) using *n*-hexadecane as an internal standard.

From first inspection of the data in Table 3, the most desirable results are obtained using high temperature and high air pressure (entries 10, 11, 16). It was therefore unsurprising that mostly low yields were achieved at milder temperature and pressure (entries 3, 5, 9). This may be explained by the high thermodynamic stability of C(sp^3)–C(sp^3) bonds thus making the reaction inaccessible without significant heating. Notably, entries 4 and 6 reveal the possibility to achieve good product yields under just 10 bar air pressure, thereby benefitting both convenience and safety. The analysis of variance (ANOVA) table (Table S11) was consistent with the observation that temperature and pressure were favorable towards the yield of **2b**. In fact, the ANOVA identified three factors as being statistically significant in the reaction (i.e. *p*-values <0.05 under the null hypothesis), these being: catalyst loading, temperature, and pressure. In other words, the high-level conditions for these three factors generated the best results. Whilst the presence of TEMPO and pyridine had proven to be beneficial in the reaction, variation from 10 to 30 mol% had no statistically significant impact on the yield of **2b**.

Based on the results vide supra, the decision was made to try to explore higher temperatures and pressures, as well as greater amounts of TEMPO and pyridine in solution. In all cases, catalyst loading was maintained at 10 mol% (see Tables S12 & S13). Notably, the harsher conditions employed were in fact disadvantageous and could not reach the yield of 60% of **2b** obtained in the first DoE screen.

Using the optimization process outlined above allowed us to isolate derivatized morpholines and derivatized diphenylpiperazine in good yields (up to 70%), as shown in Table 4. It is noteworthy to highlight that such reactivity could not be realized with our previously reported

Table 1
Influence of Pyridine Ligands on the Benchmark Reaction.

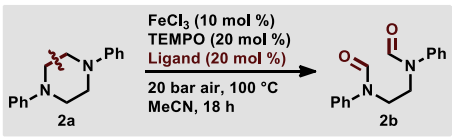

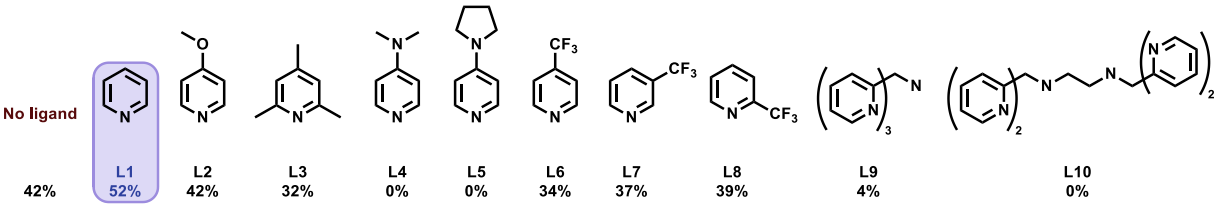

[a]Reaction conditions: **2a** (0.25 mmol), $FeCl_3$ (10 mol%), TEMPO (20 mol%), ligand (20 mol%) in MeCN (2 mL), 20 bar air, 100 °C. Yields determined by GC-FID using *n*-hexadecane as an internal standard.

Table 2
Reaction Conditions Selected for DoE Analysis of Oxidative Cleavage of **2a** Using $FeCl_3$.

factor	low level (−)	high level (+)
catalyst loading (mol%)	3	15
temperature (°C)	80	120
air pressure (bar)	10	30
pyridine loading (mol%)	10	30
TEMPO loading (mol%)	10	30

Table 3
Results of the Initial DoE Screen for Oxidative Cleavage of **2a**[a].

entry	catalyst loading (mol%)	TEMPO (mol%)	pyridine (mol%)	air pressure (bar)	temperature (°C)	yield[b] (%)
1	3	10	10	10	120	25
2	15	10	10	10	80	38
3	3	30	10	10	80	5
4	15	30	10	10	120	45
5	3	10	30	10	80	7
6	15	10	30	10	120	52
7	3	30	30	10	120	30
8	15	30	30	10	80	33
9	3	10	10	30	80	12
10	15	10	10	30	120	59
11	3	30	10	30	120	56
12	15	30	10	30	80	52
13	3	10	30	30	120	41
14	15	10	30	30	80	36
15	3	30	30	30	80	16
16	15	30	30	30	120	60
17	9	20	20	20	100	51[c]
18	9	20	20	20	100	44[c]
19	9	20	20	20	100	40[c]
20	9	20	20	20	100	45[c]

[a] Reaction conditions: 2a (0.25 mmol), $FeCl_3$ (3–15 mol%), TEMPO (10–30 mol%), pyridine (10–30 mol%) in MeCN (2 mL), 10–30 bar air, 80–120 °C. [b] Yields determined by GC-FID using *n*-hexadecane as an internal standard. [c] Center point conditions.

catalytic systems.

The high activity of this benign system is further illustrated by the lack of any noticeable induction period, leading to rapid conversion of starting material and a 13% yield of **2b** after just 30 min of reaction time. Furthermore, after 8 h full conversion is observed for the model reaction and the desired product is obtained in up to 60% yield, with no detectable co-product formation.

During the benchmark reaction, the formation of a brown solid was observed which proved to be somewhat catalytically active, capable of furnishing a 9% yield of **2b** after reaction overnight (see Supporting Information).

Table 4
C–C Bond Cleavage Reactions

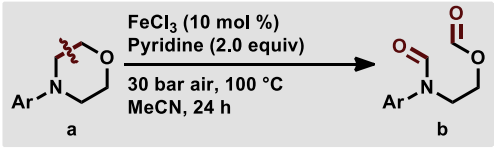

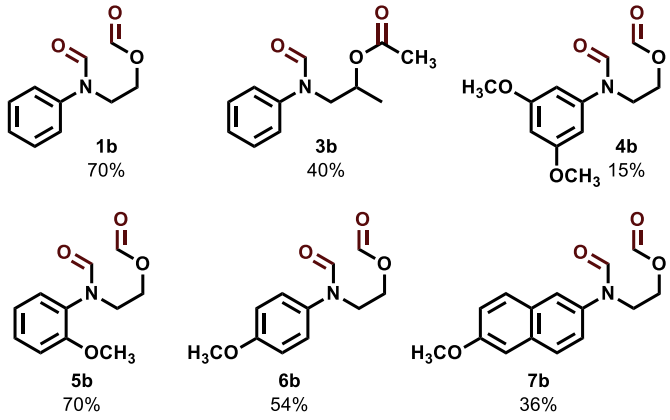

[a]Reaction conditions: **a** (0.5 mmol), $FeCl_3$ (10 mol%), pyridine (2.0 equiv) in MeCN (2 mL), 30 bar air, 100 °C, isolated yield.

Scanning transmission electron microscopy (STEM) together with electron energy loss spectroscopy (EELS) was performed to reveal the nature of this precipitate (Figs. 3 & S1). The iron oxide particles are found on a bulk phase which was proved to consist mainly of carbon, but also contains some nitrogen and tiny amounts of iron.

4. Conclusions

In conclusion, a convenient iron-based catalyst is shown to be effective for the site-selective cleavage of $C(sp^3)$–$C(sp^3)$ bonds in diphenylpiperazine and derivatized morpholines. The activation of unstrained and highly inert sp^3-hybridized centers to sp^2-hybridized aldehyde motifs unlocks the potential for new functionalization of such molecules. The use of air in this reaction is ideal as an oxidant. To the best of our knowledge, this is the first example of a competent iron-based catalytic system for the cleavage of $C(sp^3)$–$C(sp^3)$ bonds in unstrained *N*-compounds. DoE provided a rapid and effective analysis of a complex C (sp^3)–C(sp^3) bond cleaving reaction involving five variables. Three

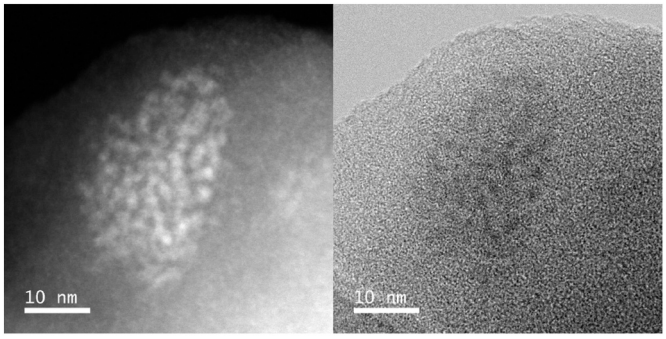

Fig. 3. STEM HAADF (left) and STEM ABF (right) images of the precipitate formed during the reaction. A group of iron oxide particles (see the brighter parts in the left image) can be seen on the bulky phase, which contains mainly carbon.

variables—temperature, air pressure and catalyst loading—were found to be significant in this reaction (i.e. p-values <0.05 under the null hypothesis). Whilst the catalyst proved more active in the presence of TEMPO and pyridine, the amount of these additives was not found to be statistically significant (p-values >0.05) in the region of chemical space explored in the factorial design.

Credit author statement

David K. Leonard: Conceptualization, data curation, investigation, writing - original draft, writing - review & editing. **Wu Li:** Conceptualization, data curation, investigation, writing - review & editing. **Nils Rockstroh:** Data curation, investigation, writing - original draft, writing - review & editing. **Kathrin Junge:** Supervision, conceptualization, writing - review & editing. **Matthias Beller:** Supervision, conceptualization, writing - review & editing.

Declaration of Competing Interest

Authors declare that they have no competing interests.

Acknowledgments

We gratefully acknowledge the support from the Federal Ministry of Education and Research (BMBF) and the State of Mecklenburg-Vorpommern. Financial support by Fonds der Chemischen Industrie (Kekulé-Stipendium n. 103231) for D.K.L. is also acknowledged. We are grateful to Dr. Pavel Ryabchuk (Galapagos NV) for his valuable contribution of ideas to the project. We thank the analytical staff of the Leibniz Institute for Catalysis, Rostock, for their excellent service.

Appendix A. Supplementary data

Supplementary data to this article can be found online at https://doi.org/10.1016/j.catcom.2021.106333.

References

[1] A. Fürstner, Iron catalysis in organic synthesis: a critical assessment of what it takes to make this base metal a multitasking champion, ACS Cent. Sci. 2 (2016) 778–789.
[2] E. de Smit, B.M. Weckhuysen, The renaissance of iron-based Fischer–Tropsch synthesis: on the multifaceted catalyst deactivation behaviour, Chem. Soc. Rev. 37 (2008) 2758–2781.
[3] M.M. Rodriguez, E. Bill, W.W. Brennessel, P.L. Holland, N_2 reduction and hydrogenation to ammonia by a molecular iron–potassium complex, Science 334 (2011) 780–783.
[4] T. Rayment, R. Schlögl, J.M. Thomas, G. Ertl, Structure of the ammonia synthesis catalyst, Nature 315 (1985) 311–313.
[5] I. Bauer, H.J. Knölker, Iron catalysis in organic synthesis, Chem. Rev. 115 (2015) 3170–3387.
[6] T.B. Boit, A.S. Bulger, J.E. Dander, N.K. Garg, Activation of C–O and C–N bonds using non-precious-metal catalysis, ACS Catal. 10 (2020) 12109–12126.
[7] A. Guðmundsson, J.-E. Bäckvall, On the use of iron in organic chemistry, Molecules. 25 (2020) 1349.
[8] Y. Lee, N.P. Mankad, J.C. Peters, Triggering N_2 uptake via redox-induced expulsion of coordinated NH_3 and N_2 silylation at trigonal bipyramidal iron, Nat. Chem. 2 (2010) 558–565.
[9] P. Hu, M. Tan, L. Cheng, H. Zhao, R. Feng, W.-J. Gu, W. Han, Bio-inspired iron-catalyzed oxidation of alkylarenes enables late-stage oxidation of complex methylarenes to arylaldehydes, Nat. Commun. 10 (2019) 2425.
[10] G. Jin, G.W. Werncke, Y. Escudié, S. Sabo-Etienne, S. Bontemps, Iron-catalyzed reduction of CO_2 into methylene: formation of C–N, C–O, and C–C bonds, J. Am. Chem. Soc. 137 (2015) 9563–9566.
[11] S. Budweg, Z. Wei, H. Jiao, K. Junge, M. Beller, Iron–PNP-pincer-catalyzed transfer dehydrogenation of secondary alcohols, ChemSusChem 12 (2019) 2988–2993.
[12] D.-S. Kim, W.-J. Park, C.-H. Jun, Metal–organic cooperative catalysis in C–H and C–C bond activation, Chem. Rev. 117 (2017) 8977–9015.
[13] L. Souillart, N. Cramer, Catalytic C–C bond activations via oxidative addition to transition metals, Chem. Rev. 115 (2015) 9410–9464.
[14] S.P. Morcillo, Radical-promoted C−C bond cleavage: a deconstructive approach for selective functionalization, Angew. Chem. Int. Ed. 58 (2019) 14044–14054.
[15] X. Wen, X. Li, X. Luo, W. Wang, S. Song, N. Jiao, Intramolecular Csp^3–H/C–C bond amination of alkyl azides for the selective synthesis of cyclic imines and tertiary amines, Chem. Sci. 11 (2020) 4482–4487.
[16] B. Wang, M.A. Perea, R. Sarpong, Transition metal-mediated C–C single bond cleavage: making the cut in total synthesis, Angew. Chem. Int. Ed. 59 (2020) 18898–18919.
[17] M. Murakami, N. Ishida, Cleavage of carbon–carbon σ-bonds of four-membered rings, Chem. Rev. 121 (2021) 264–299.
[18] R. Criegee, Eine Oxydative Spaltung von Glykolen, Ber. Dtsch. Chem. Ges. B 64 (1931) 260.
[19] L. Malaprade, Bull. Soc. Chim. Fr. 3 (1934) 833.
[20] W. Li, W. Liu, D.K. Leonard, J. Rabeah, K. Junge, A. Brückner, M. Beller, Practical catalytic cleavage of $C(sp^3)$−$C(sp^3)$ bonds in amines, Angew. Chem. Int. Ed. 58 (2019) 10693–10697.
[21] D.K. Leonard, W. Li, K. Junge, M. Beller, Improved bimetallic cobalt–manganese catalysts for selective oxidative cleavage of morpholine derivatives, ACS Catal. 9 (2019) 11125–11129.
[22] S.A. Weissman, N.G. Anderson, Design of experiments (DoE) and process optimization. A review of recent publications, Org. Process. Res. Dev. 19 (2015) 1605–1633.
[23] D. Lendrem, M. Owen, S. Godbert, DOE (Design of Experiments) in development chemistry: potential obstacles, Org. Process. Res. Dev. 5 (2001) 324–327.
[24] P. Anastas, N. Eghbali, Green chemistry: principles and practice, Chem. Soc. Rev. 39 (2010) 301–312.
[25] V.K. Aggarwal, A.C. Staubitz, M. Owen, Optimization of the Mizoroki–heck reaction using Design of Experiments (DoE), Org. Process. Res. Dev. 10 (2006) 64–69.
[26] R.A.F. Tomás, J.C.M. Bordado, J.F.P. Gomes, p-Xylene oxidation to terphthalic acid: a literature review oriented toward process optimization and development, Chem. Rev. 113 (2013) 7421–7469.
[27] J. Smidt, W. Hafner, R. Jira, J. Sedlmeier, R. Sieber, R. Rüttinger, H. Kojer, Katalytische Umsetzungen von Olefinen an Platinmetall-Verbindungen Das Consortium-Verfahren zur Herstellung von Acetaldehyd, Angew. Chem. 71 (1959) 176–182.
[28] A. Gavriilidis, A. Constantinou, K. Hellgardt, K.K. Hii, G.J. Hutchings, G.L. Brett, S. Kuhn, S.P. Marsden, Aerobic oxidations in flow: opportunities for the fine chemicals and pharmaceuticals industries, React. Chem. Eng. 1 (2016) 595–612.
[29] P.M. Osterberg, J.K. Niemeier, C.J. Welch, J.M. Hawkins, J.R. Martinelli, T. E. Johnson, T.W. Root, S.S. Stahl, Experimental limiting oxygen concentrations for nine organic solvents at temperatures and pressures relevant to aerobic oxidations in the pharmaceutical industry, Org. Process. Res. Dev. 10 (2014) 1537–1543.
[30] (a) Sigma–Aldrich Acetonitrile Safety Data Sheet. https://www.sigmaaldrich.com/MSDS/MSDS/DisplayMSDSPage.do?country=GB&language=en&productNumber=34851&brand=SIGALD&PageToGoToURL=https%3A%2F%2Fwww.sigmaaldrich.com%2Fcatalog%2Fproduct%2Fsigald%2F34851%3Flang%3Den (accessed January 12, 2020);
(b) INEOS Acetonitrile Safe Storage and Handling Guide.. https://www.ineos.com/globalassets/ineos-group/businesses/ineos-nitriles/she/2007_acetonitrile_brochure.pdf (accessed January 12, 2020).
[31] S.S. Stahl, Palladium-catalyzed oxidation of organic chemicals with O_2, Science 309 (2005) 1824–1826.
[32] D. Wang, A.B. Weinstein, P.B. White, S.S. Stahl, Ligand-promoted palladium-catalyzed aerobic oxidation reactions, Chem. Rev. 118 (2018) 2636–2679.
[33] Minitab 19. https://www.minitab.com (accessed December 14, 2020).
[34] D. Ma, Q. Cai, H. Zhang, Mild method for Ullmann coupling reaction of amines and aryl halides, Org. Lett. 5 (2003) 2453–2455.